5-1-2015

Reconciling and Validating the Cloud Thickness and Liquid Water Path Tendencies

Mohamed S. Ghonima
University of California

Joel R. Norris
University of California

Thijs Heus
Cleveland State University, t.heus@csuohio.edu

Jan Kleissl
University of California

Reconciling and Validating the Cloud Thickness and Liquid Water Path Tendencies Proposed by R. Wood and J. J. van der Dussen et al.

MOHAMED S. GHONIMA

Department of Mechanical and Aerospace Engineering, University of California, San Diego, La Jolla, California

JOEL R. NORRIS

Scripps Institution of Oceanography, University of California, San Diego, La Jolla, California

THIJS HEUS

Department of Physics, Cleveland State University, Cleveland, Ohio

JAN KLEISSL

Department of Mechanical and Aerospace Engineering, University of California, San Diego, La Jolla, California

(Manuscript received 3 October 2014, in final form 6 December 2014)

ABSTRACT

A detailed derivation of stratocumulus cloud thickness and liquid water path tendencies as a function of the well-mixed boundary layer mass, heat, and moisture budget equations is presented. The derivation corrects an error in the cloud thickness tendency equation derived by R. Wood to make it consistent with the liquid water path tendency equation derived by J. J. van der Dussen et al. The validity of the tendency equations is then tested against the output of large-eddy simulations of a typical stratocumulus-topped boundary layer case and is found to be in good agreement.

1. Introduction

Stratocumulus clouds are the most common cloud type, covering approximately one-fifth of Earth's surface in the annual mean, and as such have a large impact on Earth's radiative budget (Klein and Hartmann 1993; Wood 2012). Therefore, it is important to understand the physical process that control stratocumulus cloud properties. The mixed-layer model (MLM) first proposed by Lilly (1968) has been a popular method to examine how specific physical processes impact stratocumulus cloud properties. These models are advantageous because they are computationally inexpensive and offer a quick and intuitive way to test hypotheses.

The underlying assumption of the MLM is that the stratocumulus-topped boundary layer (STBL) is well mixed; the assumption results in a zero-dimensional model that determines mixed-layer bulk properties (i.e., the STBL depth and the conserved variables: liquid water potential temperature and total water mixing ratio). Wood (2007, hereafter W07) developed an analytical equation that relates cloud thickness to the STBL depth and conserved variables of the MLM: liquid water potential temperature and total water mixing ratio. Utilizing the cloud thickness analytical equation coupled with an MLM, W07 analyzed the validity of the aerosol second indirect effect. Similarly, van der Dussen et al. (2014, hereafter VDD14) related liquid water path (LWP) to the STBL depth and the conserved variables of the MLM to determine an equilibrium value of the inversion stability parameter, beyond which a stratocumulus cloud will thin.

Both W07 and VDD14 assumed that the STBL remains well mixed as a result of the turbulence generated by longwave cooling at the top of the cloud. The liquid water lapse rate, defined as the rate

Corresponding author address: Mohamed Ghonima, 9500 Gilman Dr., EBUII – 304, La Jolla, CA 92093-0411.
E-mail: mgohinma@ucsd.edu

DOI: 10.1175/JAS-D-14-0287.1

at which liquid water mixing ratio changes with altitude, can be assumed to be adiabatic; the lapse rate is additionally assumed to be constant in height for the relatively thin stratocumulus clouds. Therefore, LWP is directly proportional to the square of the cloud thickness. However, the cloud thickness and LWP tendencies derived by W07 and VDD14, respectively, are not equivalent. The discrepancy stems from an error in W07's derivation of the cloud-base-height response to changes in heat energy in the STBL. Thus, the goal of this paper is first to provide a derivation of the cloud thickness analytical equation that corrects W07's derivation, thereby making the W07 cloud thickness tendency consistent with the VDD14 LWP tendency [provided as Eqs. (23) and (25) later]. Second, the paper uses large-eddy simulation to determine the accuracy of the LWP and cloud thickness tendency equations for a typical STBL.

2. Formulation of the cloud thickness and liquid water path tendencies

The tendencies of cloud thickness and liquid water path are formulated in terms of the two moist conserved variables: q_t is the total water mixing ratio ($q_t = q_v + q_l$), where q_v is the water vapor mixing ratio and q_l is the liquid water mixing ratio, and θ_l is the liquid water potential temperature [$\theta_l = \theta - (1/\Pi)(L_v/c_p)q_l$], where θ represents the potential temperature, $\Pi = (P/P_0)^{R_d/c_p}$ is the Exner function, L_v is the latent heat of evaporation, c_p is the specific heat of air at constant pressure, and R_d is the dry-air gas constant.

W07 alternatively formulated the tendencies in terms of total water mixing ratio and liquid water static energy ($s_l = c_pT + gz - L_vq_l$), where g is the gravitational constant and z is the altitude. Liquid water static energy is a moist conserved variable that is similar to liquid water potential temperature and can be related as $s_l = c_p\Pi\theta_l + gz$.

VDD14 arrived at the LWP tendency equation by formulating an equation for liquid water specific humidity at the top of the STBL. Here we choose to derive the equations in terms of cloud-base and inversion heights, similar to W07, as expressing the inversion height as function of the mass balance equation and having the cloud-base height respond to changes in heat and moisture content makes it easier to understand how the stratocumulus cloud layer would respond to the different physical factors such as entrainment or radiation.

The final corrected cloud thickness tendency is formulated as

$$\frac{\partial h}{\partial t} = w_e + w_s(z_i) - \mathbf{v}_H \cdot \nabla z_i - \frac{R_d T_{b,1}}{g q_t}\left(1 - \frac{L_v R_d}{c_p R_v T_{b,1}}\right)^{-1}\frac{\partial q_t}{\partial t} - \frac{c_p \Pi_{b,1}}{g}\left(1 - \frac{c_p R_v T_{b,1}}{R_d L_v}\right)^{-1}\frac{\partial \theta_L}{\partial t},$$

and the final LWP tendency equation, equivalent to VDD14's Eq. (9), is expressed as

$$\frac{1}{\overline{\rho}_{\text{air}} h}\frac{\partial \text{LWP}}{\partial t} = -\Gamma_{q_l}[w_e + w_s(z_i) - \mathbf{v}_H \cdot \nabla z_i] + \left(1 + \frac{L_v^2 q_t}{c_p R_v T_{b,1}^2}\right)^{-1}\frac{\partial q_t}{\partial t} - \Pi_{b,1}\frac{L_v q_t}{R_v T_{b,1}^2}\left(1 + \frac{L_v^2 q_t}{c_p R_v T_{b,1}^2}\right)^{-1}\frac{\partial \theta_L}{\partial t}.$$

Section 2 provides a detailed derivation of the above tendency equations. Two key assumptions are made in the following derivation of the cloud thickness and LWP tendencies: 1) the STBL is well mixed and 2) the STBL height is sufficiently shallow such that variations in the density of air are negligible.

a. *Cloud thickness and liquid water path*

LWP is defined as

$$\text{LWP} = \int_0^{z_i} \overline{\rho}_{\text{air}} q_l \, dz = \int_{z_b}^{z_i} \overline{\rho}_{\text{air}} q_l \, dz, \qquad (1)$$

where $\overline{\rho}_{\text{air}}$ represents the total density of air (assumed to be constant across the depth of the STBL) and z_b and z_i represent cloud-base height and inversion-base height, respectively. Parcels in the cloud layer are assumed to ascent adiabatically from the cloud base to top. Hence, the liquid water mixing ratio, for the relatively thin stratocumulus cloud, is assumed to increase linearly with height z above the cloud base. Nicholls and Leighton (1986) and Albrecht et al. (1990) showed that the observed cloud water content was generally close to the adiabatic value in well-mixed boundary layers. Although the constant liquid water lapse rate is not observed universally, it has been thoroughly documented in in measurement campaigns such as DYCOMS (Stevens et al. 2003b) and in the high-resolution Cloud Feedbacks Model Intercomparison Project (CFMIP)/Global Atmospheric System Studies (GASS) Intercomparison of Large-Eddy and Single-Column Models (CGILS) simulations (Blossey et al.

2013). Liquid water mixing ratio can then be expressed as

$$q_l(z) = -\Gamma_{q_l} z, \tag{2}$$

where $\Gamma_{q_l}(p, T) = -\partial q_l/\partial z$ is the lapse rate of liquid water mixing ratio. The LWP tendency can be expressed as

$$\mathrm{LWP} = \int_{z_b}^{z_i} (-\overline{\rho}_{\mathrm{air}}\Gamma_{q_l} z\, dz) = -\frac{1}{2}\overline{\rho}_{\mathrm{air}}\Gamma_{q_l} h^2,$$

$$\frac{\partial \mathrm{LWP}}{\partial t} = -\overline{\rho}_{\mathrm{air}}\Gamma_{q_l} h \frac{\partial h}{\partial t}. \tag{3}$$

Next, the temporal evolution of cloud thickness h can be formulated as

$$\frac{\partial h}{\partial t} = \frac{\partial z_i}{\partial t} - \frac{\partial z_b}{\partial t}. \tag{4}$$

b. Inversion height from mass balance

Assuming again constant total air density up to the inversion height, the columnar mass m_{clm} is formulated in terms of the STBL inversion height as $m_{\mathrm{clm}} = \overline{\rho}_{\mathrm{air}} z_i$. Therefore, the inversion height tendency can be formulated in terms of the columnar mass balance equation as

$$\frac{\partial z_i}{\partial t} + \mathbf{v}_H \cdot \nabla z_i = w_e + w_s(z_i), \tag{5}$$

where $\overline{\rho}_{\mathrm{air}}$ cancelled out on both sides of the equation, w_e represents the entrainment rate, and w_s is the vertical large-scale wind component. The second term on the left-hand side of Eq. (5) represents large-scale horizontal advection through the STBL column. This term is ignored in both W07 and VDD14, which would be valid in a Lagrangian approach to the cloud field. However, we will see that the term only adds a trivial term to the resulting equations.

c. Cloud-base height from energy and moisture

Cloud-base height, which also corresponds to the lifting condensation level (LCL), is defined as the height where the saturation mixing ratio q_s is equal to the total water mixing ratio,

$$q_{sb}(T_b, p_b) = q_t, \tag{6}$$

where T_b and p_b are the temperature and pressure values, respectively, evaluated at the cloud-base height. The tendency of the cloud-base height can be formulated in terms of liquid water potential temperature and total water mixing ratio as

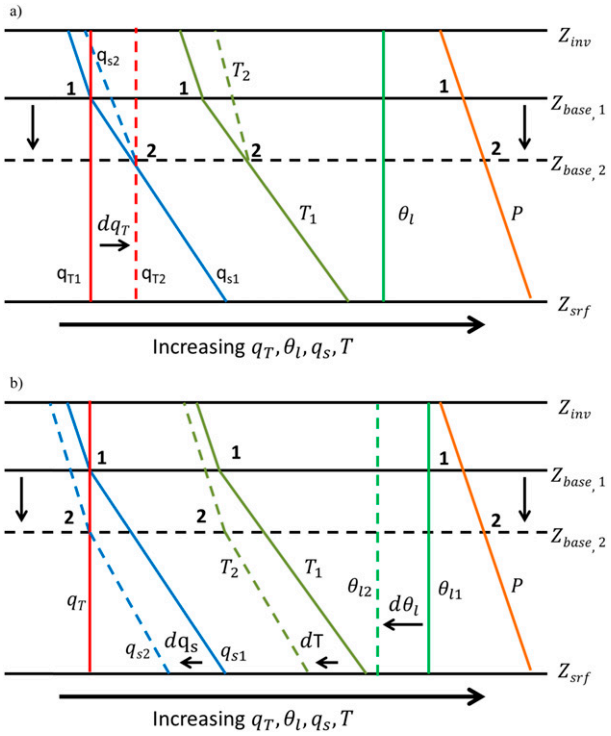

FIG. 1. Response of cloud-base height and temperature and humidity profiles to (a) an increase in total water mixing ratio and (b) a decrease in liquid water potential temperature. Solid lines (''1'') show initial profiles and dashed lines (''2'') show the response.

$$\frac{\partial z_b}{\partial t} = \frac{\partial z_b}{\partial \theta_l}\frac{\partial \theta_l}{\partial t} + \frac{\partial z_b}{\partial q_t}\frac{\partial q_t}{\partial t}. \tag{7}$$

Note that in the STBL, the conserved variables (θ_l, q_t) are constant with height; however, other thermodynamic variables such as q_s and T are not. Hence, the subscript b is added to denote that the variable is evaluated at the cloud-base height.

1) Change in STBL moisture content at constant heat content

Consider a case where there is a change in total water mixing ratio dq_t and liquid water potential temperature is kept constant ($d\theta_l = 0$, Fig. 1a). In this case, moisture is added to the STBL, thus shifting the q_t profile to the right, while total heat in the STBL remains constant. From the definition of cloud-base height, dq_t is equal to the change in saturation mixing ratio at the cloud base,

$$dq_t = dq_s(T_b, p_b). \tag{8}$$

The total differential of the saturation mixing ratio can be expressed as

$$dq_t = dq_s(T_b, p_b) = \frac{\partial q_s}{\partial T} dT + \frac{\partial q_s}{\partial P} dp. \tag{9}$$

Thus, the response of cloud-base height z_b to a change in the total water mixing ratio is formulated as

$$\frac{dq_t}{dz_b} = \frac{dq_s(T_b, p_b)}{dz_b} = \frac{\partial q_{s_b}}{\partial T_b}\frac{dT_b}{dz_b} + \frac{\partial q_{s_b}}{\partial p_b}\frac{dp_b}{dz_b}, \tag{10}$$

where $dT_b = T_{b,2} - T_{b,1}$ is the temperature difference evaluated at the initial (subscript 1) and response (subscript 2) cloud bases and $dp_b = p_{b,2} - p_{b,1}$. Henceforth, subscript b,1 denotes that the thermodynamic variable is evaluated at the initial cloud base and subscript b,2 denotes that it is evaluated at the response or final cloud base. The temperature profile in the cloud layer will shift as a result of condensation (evaporation) of cloud water droplets due to the addition (subtraction) of moisture from the STBL (Fig. 1a).

Taking the derivative of the saturation mixing ratio $\{q_s = \varepsilon[e_s/(p - e_s)]$, where e_s is the saturation pressure$\}$ with respect to temperature results in $\partial q_s/\partial T = \varepsilon(\partial e_s/\partial T)(1/p)(1 + e_s/p)$, where ε represents the ratio of water vapor to dry-air average molecular weight ($\varepsilon = M_v/M_d = 0.622$). Utilizing the Clausius–Clapeyron equation ($\partial e_S/\partial T = L_v e_s/R_v T^2$) and assuming that $e_s/p \ll 1$:

$$\frac{\partial q_s}{\partial T} = \frac{L_v q_t}{R_v T_{b,1}^2}, \tag{11}$$

where R_v represents the water vapor gas constant. Since there is no change in the total heat content of the STBL (Fig. 1b), the temperature profiles below the cloud layer do not shift. Hence, the dry adiabatic lapse rate can be utilized to formulate dT_b/dz_b as

$$\frac{dT_b}{dz_b} = -\frac{g}{c_p}. \tag{12}$$

Taking the partial derivative of the saturation mixing ratio with respect to pressure and again assuming that $p \gg e_s$,

$$\frac{\partial q_s}{\partial p} \approx -\frac{q_t}{p}. \tag{13}$$

Assuming the atmosphere is in hydrostatic balance,

$$\frac{dp}{dz} \approx -\frac{pg}{R_d T}. \tag{14}$$

Next, substituting Eqs. (11)–(14) into Eq. (10), an equation is obtained for the response of cloud-base height to a change in STBL moisture content

$$\frac{dz_b}{dq_t} = \frac{R_d T_{b,1}}{g q_t}\left(1 - \frac{L_v R_d}{c_p R_v T_{b,1}}\right)^{-1}. \tag{15}$$

Equation (15) is equivalent to the one derived by W07 [their Eq. (A3)].

2) Change in STBL heat content at constant moisture content

Next, a case is considered in which the liquid water potential temperature changes $d\theta_l$ through the removal of heat in the STBL and the total water mixing ratio is kept constant ($dq_t = 0$); that is, no moisture is added or removed from the STBL (Fig. 1b). Thus, the removal (addition) of heat results in the cloud liquid water condensing (evaporating) thereby decreasing (increasing) the cloud-base height. The total differential of the liquid water potential temperature can be expressed as

$$d\theta_l = \frac{\partial \theta_l}{\partial T} dT + \frac{\partial \theta_l}{\partial p} dp. \tag{16}$$

Note that $q_l = 0$ at cloud base, $d\theta_l$ is constant in height since it is conserved in the well-mixed STBL, and the temperature difference dT varies in altitude. Evaluating $d\theta_l$ at the cloud base,

$$\frac{d\theta_l}{dz_b} = \frac{1}{\Pi_{b,1}}\frac{dT_b}{dz_b} - \frac{T_{b,1}}{\Pi_{b,1}^2}\frac{d\Pi_b}{dz_b}, \tag{17}$$

where $d\Pi_b = \Pi_{b,2} - \Pi_{b,1}$ is the Exner function difference evaluated at the two cloud bases. It is important to note that dT_b does not follow either the dry or moist adiabatic lapse rate as the vertical temperature profile is shifted owing to the removal of heat in the STBL (Fig. 1b). Utilizing the definition of the Exner function and assuming the atmosphere is in hydrostatic balance [Eq. (14)], Eq. (17) is can be simplified as

$$\begin{aligned}\frac{d\theta_l}{dz_b} &= \frac{1}{\Pi_{b,1}}\frac{dT_b}{dz_b} - \frac{R_d T_{b,1}}{c_p p_{b,1}\Pi_{b,1}}\frac{dp_b}{dz_b} \\ &= \frac{1}{\Pi_{b,1}}\left(\frac{dT_b}{dz_b} + \frac{g}{c_p}\right).\end{aligned} \tag{18}$$

In the present case q_t remains constant; therefore, q_s at the initial cloud base and the response cloud base remains constant as well ($q_t = q_{s_{b,1}} = q_{s_{b,2}}$). The saturation mixing ratio at the cloud base can then be expressed as $q_{s_{b,1}} = \varepsilon \times (e_{s_{b,1}}/p_{b,1}) = \varepsilon \times (e_{s_{b,2}}/p_{b,2})$. Hence, $de_{s_b}/e_{s_{b,1}} = dp_b/p_{b,1}$. Utilizing the definition of the saturation water vapor pressure $\{e_s = e_{s,\mathrm{tr}} \exp[(L_v/R_v)(1/T_{\mathrm{tr}} - 1/T)]$, where $e_{s,\mathrm{tr}}$ and T_{tr} are the saturation pressure and temperature, respectively, evaluated at the triple point$\}$

and the hydrostatic balance assumption [Eq. (14)], an expression for dT_b/dz_b is derived as

$$\begin{aligned} de_{s_b} &= e_{s,\mathrm{tr}}\frac{L_v}{R_v T_{b,1}^2}\exp\left[\frac{L_v}{R_v}\left(\frac{1}{T_{\mathrm{tr}}}-\frac{1}{T_{b,1}}\right)\right]dT_b \\ &= \frac{L_v e_{s_{b,1}}}{R_v T_{b,1}^2}dT_b, \\ \frac{de_{s_b}}{e_{s_{b,1}}} &= \frac{dp_b}{p_{b,1}} = -\frac{g}{R_d T_{b,1}}dz_b, \\ \frac{de_{s_b}}{e_{s_{b,1}}} &= \frac{L_v}{R_v T_{b,1}^2}dT_b = -\frac{g}{R_d T_{b,1}}dz_b, \\ \frac{dT_b}{dz_b} &= -\frac{gR_v T_{b,1}}{R_d L_v}. \end{aligned} \tag{19}$$

Substituting Eq. (19) into (18), an equation is obtained for the response of cloud-base height to a change in STBL heat content,

$$\frac{dz_b}{d\theta_l} = \frac{c_p\Pi_1}{g}\left(1-\frac{c_p R_v T_{b,1}}{R_d L_v}\right)^{-1}. \tag{20}$$

To compare this response of cloud-base height to changes in STBL heat content with the response derived by W07, Eq. (20) is reformulated in terms of liquid water static energy instead of liquid water potential temperature,

$$\begin{aligned} \frac{ds_l}{dz_b} &= c_p\frac{dT_b}{dz_b}+g, \\ \frac{dz_b}{ds_l} &= \frac{1}{g}\left(1-\frac{c_p R_v T_{b,1}}{R_d L_v}\right)^{-1}, \end{aligned} \tag{21}$$

where $dq_l = 0$ at the cloud base and Eq. (19) was substituted for dT_b/dz_b. Contrastingly, W07 derived the response of cloud base to changes in liquid water static energy as $dz_b/ds_l = (\partial z_b/\partial T_b)(\partial T_b/\partial s_l) = 1/g$ [W07, Eq. (A5)]. W07 assumed that the change in cloud-base temperature followed the dry adiabatic lapse rate as the height of cloud base changed and neglected the fact that the temperature profile also shifts because of the addition or removal of heat to the STBL (Fig. 1b). As such, Eq. (19) should be used to compute dT_b/dz_b rather than the dry adiabatic lapse rate. Additionally, W07 neglected that the cloud-base height or the LCL is a function of both temperature and pressure. The resulting omission of $[1-(c_p R_v T_{b,1}/R_d L_v)]^{-1}$ introduces an error of about 22% to the cloud-base response to changes in STBL heat content for a typical cloud-base temperature $T_{b,1}$ of 286 K.

d. *Reconciling cloud thickness and liquid water path tendencies*

To obtain the temporal evolution of cloud-base height in response to changes in moisture or heat content, Eqs. (15) and (20) are substituted into Eq. (7):

$$\begin{aligned} \frac{\partial z_b}{\partial t} &= \frac{R_d T_{b,1}}{g q_t}\left(1-\frac{L_v R_d}{c_p R_v T_{b,1}}\right)^{-1}\frac{\partial q_t}{\partial t} \\ &\quad + \frac{c_p\Pi_{b,1}}{g}\left(1-\frac{c_p R_v T_{b,1}}{R_d L_v}\right)^{-1}\frac{\partial \theta_L}{\partial t}. \end{aligned} \tag{22}$$

Utilizing Eqs. (4), (5), and (22), the cloud thickness tendency can be expressed as

$$\begin{aligned} \frac{\partial h}{\partial t} &= w_e + w_s(z_i) - \mathbf{v}_H\cdot\nabla z_i \\ &\quad - \frac{R_d T_{b,1}}{g q_t}\left(1-\frac{L_v R_d}{c_p R_v T_{b,1}}\right)^{-1}\frac{\partial q_t}{\partial t} \\ &\quad - \frac{c_p\Pi_{b,1}}{g}\left(1-\frac{c_p R_v T_{b,1}}{R_d L_v}\right)^{-1}\frac{\partial \theta_L}{\partial t}. \end{aligned} \tag{23}$$

And similarly substituting the above equation into Eq. (3), the LWP tendency can be formulated as

$$\begin{aligned} \frac{-1}{\overline{\rho}_{\mathrm{air}} h\Gamma_{q_l}}\frac{\partial \mathrm{LWP}}{\partial t} &= w_e + w_s(z_i) - \mathbf{v}_H\cdot\nabla z_i \\ &\quad - \frac{R_d T_{b,1}}{g q_t}\left(1-\frac{L_v R_d}{c_p R_v T_{b,1}}\right)^{-1}\frac{\partial q_t}{\partial t} \\ &\quad - \frac{c_p\Pi_{b,1}}{g}\left(1-\frac{c_p R_v T_{b,1}}{R_d L_v}\right)^{-1}\frac{\partial \theta_L}{\partial t}. \end{aligned} \tag{24}$$

VDD14 arrived at the LWP tendency equation by formulating an equation for liquid water specific humidity at the top of the STBL rather than in terms of cloud-base and inversion heights. Multiplying the liquid water mixing ratio lapse rate [Eq. (A.3)] into both sides of Eq. (24), the LWP tendency can be expressed as

$$\begin{aligned} \frac{1}{\overline{\rho}_{\mathrm{air}} h}\frac{\partial \mathrm{LWP}}{\partial t} &= -\Gamma_{q_l}[w_e + w_s(z_i) - \mathbf{v}_H\cdot\nabla z_i] \\ &\quad + \left(1+\frac{L_v^2 q_t}{c_p R_v T_{b,1}^2}\right)^{-1}\frac{\partial q_t}{\partial t} \\ &\quad - \Pi_{b,1}\frac{L_v q_t}{R_v T_{b,1}^2}\left(1+\frac{L_v^2 q_t}{c_p R_v T_{b,1}^2}\right)^{-1}\frac{\partial \theta_L}{\partial t}. \end{aligned} \tag{25}$$

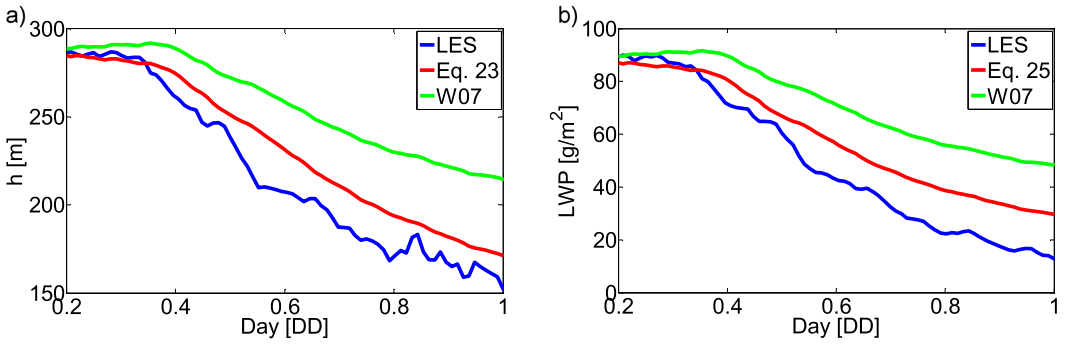

FIG. 2. (a) Cloud thickness for the nocturnal DYCOMS case and (b) LWP. Blue lines represent LES results and red lines represent the analytical Eq. (23) for cloud thickness and Eq. (25) for LWP. The green line represents the cloud thickness computed using W07's Eqs. (1), (2), (A4), and (A5).

Equation (25) is equivalent VDD14's Eq. (9) except for the large-scale horizontal advection term ($\mathbf{v}_H \cdot \nabla z_i$), which VDD14 neglected.

3. Validation

To test how well the analytical equation of cloud thickness tendency performs, Eq. (23) was applied to two cases:

1) The first research flight (RF01) of DYCOMS-II (Stevens et al. 2003b) in a nocturnal STBL. The STBL was within the buoyancy reversal regime, which made the cloud deck particularly susceptible to dissolution due to run-away entrainment, which, in turn, made the simulations challenging (Stevens et al. 2003a).
2) The CGILS s12 case, which consists of a typical well-mixed stratocumulus over cool sea surface

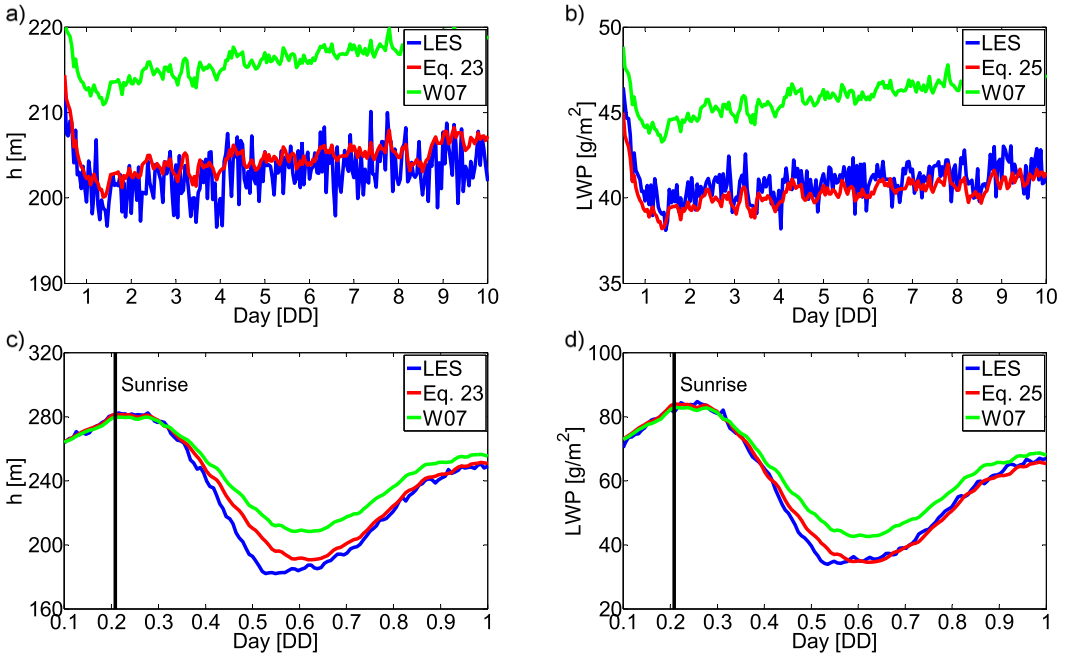

FIG. 3. (left) Cloud thickness for CGILS s12 case with (a) constant solar loading and (c) diurnally varying solar loading. (right) LWP for CGILS s12 case with (b) constant solar loading and (d) diurnally varying solar loading. Blue lines represent LES results and red lines represent the analytical Eq. (23) for cloud thickness and Eq. (25) for LWP. The green line represents the cloud thickness computed using W07's Eqs. (1), (2), (A4), and (A5). The solid vertical lines in (b) and (d) correspond to the time at sunrise.

temperatures off the coast of California in June (Zhang et al. 2012).

In both cases, the mass, energy, and moisture tendencies of the STBL were obtained from output of the University of California, Los Angeles (UCLA) large-eddy simulation (LES; Stevens et al. 2005). The LES tendencies were then used as input to Eqs. (23) and (24) to compute the cloud thickness and LWP tendencies, respectively.

For the DYCOMS case, the vertical grid spacing is 5 m near the surface and the inversion with grid stretching in between and above the inversion, and the horizontal grid resolution is 50 m (Stevens et al. 2005). The CGILS case has vertical grid spacing that is 10 m near the surface and refined (10% per layer) to obtain a 5-m resolution near the inversion after which the grid is stretched again and the horizontal grid spacing was set at 25 m (Blossey et al. 2013). The cloud water content is a diagnostic variable based on the supersaturation, the cloud droplet number concentration is prescribed, and the droplets evolve into raindrops under the actions of the ambient flow and microphysical processes such as accretion and sedimentation (Seifert and Beheng 2006). An interactive radiation scheme was used for the CGILS case (Pincus and Stevens 2009). For the DYCOMS case, a parameterized radiation scheme was used (Stevens et al. 2003a). Very little impact on the BL evolution is therefore expected.

Note that unlike in W07 and VDD14, the analytical equation for cloud thickness tendency was not coupled to an MLM. Instead, the mass, energy, and moisture tendencies were obtained from the LES output as the goal of this paper is to provide a correct derivation of the cloud thickness tendency and not to test the validity of an MLM in simulating the STBL.

The cloud thickness derived from the analytical equation h^a is compared with the cloud thickness obtained from LES output h^{ref} for the DYCOMS case, which consisted of a 24-h period without solar loading (Fig. 2) and two variations of the CGILS s12 case: 1) steady, monthly-averaged forcing and solar loading run to equilibrium (10-day simulation), and 2) steady, monthly-averaged forcing and realistic, diurnally varying solar loading run for 24 h (Fig. 3). The mean-bias error (MBE) and root-mean-square error (RMSE) were compared for both cases in Table 1, where $\mathrm{MBE} = (\sum_{t=1}^{N} h_t^a - h_t^{\mathrm{ref}})/N$ and $\mathrm{RMSE} = \sqrt{[\sum_{t=1}^{N}(h_t^a - h_t^{\mathrm{ref}})^2]/N}$, and N is the sample size. The cloud thickness and LWP derived from the analytical tendency equations were found to be in good agreement with the LES output.

TABLE 1. Mean values, MBE, and RMSE are computed using the analytically derived and LES output of cloud thickness and LWP [Eqs. (23) and (25), respectively] compared to the LES output. Errors are reported for the DYCOMS case as well as for both CGILS s12 cases.

	Cloud thickness (m)			LWP (g m^{-2})		
	Mean	MBE	RMSE	Mean	MBE	RMSE
DYCOMS	231.84	7.19	14.28	58.10	7.19	9.56
CGILS case 1	204.25	1.63	2.74	41.19	−0.614	0.933
CGILS case 2	234.23	4.68	7.24	58.62	0.259	1.91

4. Conclusions

A reconciliation of cloud thickness and LWP tendencies derived by W07 and VDD14 has been presented. W07's derivation of the cloud-base-height response to changes in STBL heat content used the dry adiabatic lapse rate and neglected the fact that the temperature profile also shifts because of the addition or removal of heat to the STBL. Hence, when W07's derivation is compared with the corrected response equation [Eq. (21)], W07's derivation was found to overestimate the cloud-base-height response to changes in STBL heat content by about 22% for a typical cloud-base-height temperature of 286 K. Validation of the derived equations against LES results of the DYCOMS and CGILS s12 cases with constant and varying solar loading showed good agreement.

Following W07 and VDD14, the derived tendency equations [Eqs. (23)–(25)] can be coupled with the MLM formulation proposed by Lilly (1968). The MLM relates the heat and moisture tendencies to the different physical process occurring in the STBL, such as precipitation, entrainment, and radiation. Thus, Eqs. (23)–(25) coupled with the MLM can be utilized to study how different physical processes affect the cloud thickness.

The derived analytical Eq. (22) provides a direct relationship between cloud-base-height tendency and the heat and moisture tendencies; therefore, Eq. (22), for example, coupled with measurements of cloud-base height (e.g., with a ceilometer) could be used to validate observations of the heat and moisture budgets in the STBL. The stratocumulus cloud lifetime over land has seen renewed interest to enable accurate forecasting of solar power generation in coastal California, and the MLMs and cloud thickness tendency equations can provide insights into the importance of different terms in the moisture and heat budgets.

Acknowledgments. The authors thank the CPUC California Solar Initiative RD&D program for funding.

APPENDIX

Liquid Water Mixing Ratio Lapse Rate

Liquid water mixing ratio lapse rate can be expressed in terms of saturation pressure q_s as follows:

$$\Gamma_{q_l} = -\frac{\partial q_l}{\partial z} = \frac{\partial q_s}{\partial z} = \left(\frac{\partial q_s}{\partial T}\frac{dT}{dz} + \frac{\partial q_s}{\partial P}\frac{dp}{dz}\right). \quad \text{(A1)}$$

Next, since Eq. (A1) is evaluated in the cloud layer, the saturated adiabatic lapse rate is utilized:

$$\frac{dT}{dz} \approx -\left(\frac{g}{c_p} + \frac{L_v}{c_p}\frac{\partial q_s}{\partial z}\right). \quad \text{(A2)}$$

Finally, substituting Eqs. (11), (13), (14), and (A2) into Eq. (A1), the following equation for the liquid water mixing ratio lapse rate evaluated at the cloud base is obtained:

$$\Gamma_{q_l} = \frac{\partial q_s}{\partial z} = g\left(1 + \frac{L_v^2 q_{s_{b,1}}}{c_p R_v T_{b,1}^2}\right)^{-1}\left(\frac{q_{s_{b,1}}}{R_d T_{b,1}} - \frac{L_v q_{s_{b,1}}}{c_p R_v T_{b,1}^2}\right). \quad \text{(A3)}$$

REFERENCES

Albrecht, B. A., C. W. Fairall, D. W. Thomson, and A. B. White, 1990: Surface-based remote sensing of the observed and the adiabatic liquid water content of stratocumulus clouds. *Geophys. Res. Lett.,* **17,** 89–92, doi:10.1029/GL017i001p00089.

Blossey, P. N., and Coauthors, 2013: Marine low cloud sensitivity to an idealized climate change: The CGILS LES intercomparison. *J. Adv. Model. Earth Syst.,* **5,** 234–258, doi:10.1002/jame.20025.

Klein, S. A., and D. L. Hartmann, 1993: The seasonal cycle of low stratiform clouds. *J. Climate,* **6,** 1587–1606, doi:10.1175/1520-0442(1993)006<1587:TSCOLS>2.0.CO;2.

Lilly, D. K., 1968: Models of cloud-topped mixed layers under a strong inversion. *Quart. J. Roy. Meteor. Soc.,* **94,** 292–309, doi:10.1002/qj.49709440106.

Nicholls, S., and J. Leighton, 1986: An observational study of the structure of stratiform cloud sheets: Part I. Structure. *Quart. J. Roy. Meteor. Soc.,* **112,** 431–460, doi:10.1002/qj.49711247209.

Pincus, R., and B. Stevens, 2009: Monte Carlo spectral integration: A consistent approximation for radiative transfer in large eddy simulations. *J. Adv. Model. Earth Syst.,* **1,** 1, doi:10.3894/JAMES.2009.1.1.

Seifert, A., and K. D. Beheng, 2006: A two-moment cloud microphysics parameterization for mixed-phase clouds. Part 1: Model description. *Meteor. Atmos. Phys.,* **92** (1–2), 45–66, doi:10.1007/s00703-005-0112-4.

Stevens, B., and Coauthors, 2003a: On entrainment rates in nocturnal marine stratocumulus. *Quart. J. Roy. Meteor. Soc.,* **129,** 3469–3493, doi:10.1256/qj.02.202.

——, and Coauthors, 2003b: Dynamics and Chemistry of Marine Stratocumulus—DYCOMS-II. *Bull. Amer. Meteor. Soc.,* **84,** 579–593, doi:10.1175/BAMS-84-5-579.

——, and Coauthors, 2005: Evaluation of large-eddy simulations via observations of nocturnal marine stratocumulus. *Mon. Wea. Rev.,* **133,** 1443–1462, doi:10.1175/MWR2930.1.

van der Dussen, J. J., S. R. de Roode, and A. P. Siebesma, 2014: Factors controlling rapid stratocumulus cloud thinning. *J. Atmos. Sci.,* **71,** 655–664, doi:10.1175/JAS-D-13-0114.1.

Wood, R., 2007: Cancellation of aerosol indirect effects in marine stratocumulus through cloud thinning. *J. Atmos. Sci.,* **64,** 2657–2669, doi:10.1175/JAS3942.1.

——, 2012: Stratocumulus clouds. *Mon. Wea. Rev.,* **140,** 2373–2423, doi:10.1175/MWR-D-11-00121.1.

Zhang, M., C. S. Bretherton, P. N. Blossey, S. Bony, F. Brient, and J.-C. Golaz, 2012: The CGILS experimental design to investigate low cloud feedbacks in general circulation models by using single-column and large-eddy simulation models. *J. Adv. Model. Earth Syst.,* **4,** M12001, doi:10.1029/2012MS000182.